Journal of Applied Economics

ISSN: 1514-0326 (Print) 1667-6726 (Online) Journal homepage: www.tandfonline.com/journals/recs20

Combining deep learning with econometric models: volatility forecasting using the KAN-GARCH-MIDAS framework

Ting Liu, Weichong Choo, Han Xinping & Le Li

To cite this article: Ting Liu, Weichong Choo, Han Xinping & Le Li (2025) Combining deep learning with econometric models: volatility forecasting using the KAN-GARCH-MIDAS framework, Journal of Applied Economics, 28:1, 2555479, DOI: 10.1080/15140326.2025.2555479

To link to this article: https://doi.org/10.1080/15140326.2025.2555479

Published online: 10 Sep 2025.

JOURNAL OF APPLIED ECONOMICS
2025, VOL. 28, NO. 1, 2555479
https://doi.org/10.1080/15140326.2025.2555479

Routledge
Taylor & Francis Group

RESEARCH ARTICLE

OPEN ACCESS Check for updates

Combining deep learning with econometric models: volatility forecasting using the KAN-GARCH-MIDAS framework

Ting Liu[a,b], Weichong Choo[a], Han Xinping[c] and Le Li[a]

[a]School of Business and Economics, Universiti Putra Malaysia, Seri Kembangan, Malaysia; [b]School of Business and Trade, Henan Industry and Trade Vocational College, Zhengzhou, China; [c]School of Economics and Trade, Henan Finance University, Zhengzhou, China

ABSTRACT

Machine learning and deep learning are increasingly applied in finance, yet few studies explore how they can enhance traditional econometric models. This study proposes an innovative KAN-GM model, integrating the Kolmogorov–Arnold network (KAN) with the GARCH-MIDAS model to extract nonlinear macroeconomic features for volatility forecasting. Empirical results show that KAN-GM outperforms traditional GARCH in MAE and MedAE, consistently ranks in the optimal model set via MCS tests, and demonstrates strong cross-market adaptability (stocks and forex). It also maintains robustness pre- and post-COVID-19. The model effectively combines deep learning and econometrics, improving financial risk prediction.

ARTICLE HISTORY
Received 16 December 2024
Accepted 27 August 2025

KEYWORDS
Forecasting; volatility; GARCH-MIDAS; KAN

1. Introduction

The volatility of stock price indices affects consumers' investment behavior and returns and significantly impacts the stability of the financial environment (Yu et al., 2023). For long-term investors, volatility serves as a risk indicator that aids in decision-making. For short-term investors, the level of long-term volatility is crucial, as it determines the expected magnitude of future trends and risks. Additionally, they can adjust their trading strategies based on changes in long-term volatility (Gong et al., 2022). Meanwhile, volatility, as a key measure of equity risk, plays an essential role not only in the investment domain but also in influencing asset pricing, risk management, and macroeconomic policymaking (Poon & Granger, 2003). In general, volatility measures the variance of an asset's time-series returns over a certain period (Cizeau et al., 1997), quantifying the risk associated with that asset. Financial asset returns often exhibit clusters of volatility, where periods of "sharp" or high market volatility are followed by similarly high-volatility periods, and periods of "calm" or low market volatility are followed by low-volatility periods (Tsay, 2005). Accurate forecasting of volatility remains a key area of interest for government policymakers, financial regulators, and academics. For instance, it helps investors formulate smarter investment strategies, provides market participants with tools to guard against risks, and offers policymakers critical insights to ensure the national economy runs smoothly (Wei et al., 2021). Especially for investors, reducing forecasting errors can lower investment risks and enhance profitability (Bazrkar & Hosseini, 2023).

Numerous empirical studies show that financial time series data are often characterized by "negative skewness," "excessive kurtosis," and time persistence of conditional variances, which do not satisfy the assumption of homogeneity. In the long run, stock returns do not remain constant at the second moment. This implies that stock volatility uncertainty changes over time and is time-varying. The GARCH model developed by Bollerslev (1986) provides a powerful tool for studying stock market volatility. However, the model captures volatility on a single time scale only (Wu et al., 2022). Song et al. (2023) highlight that introducing macroeconomic variables into forecasting models can enhance forecasting accuracy. However, the frequencies of these macroeconomic variables usually do not align with the frequencies of financial

CONTACT Weichong Choo wcchoo@upm.edu.my School of Business and Economics, Universiti Putra Malaysia, Seri Kembangan, Malaysia

market data, as macroeconomic data are typically low-frequency, such as monthly, quarterly, or annual. This creates a significant challenge when incorporating frequency-inconsistent prior indicators into GARCH models (ERSİN et al., 2022). Traditional GARCH models are one-component volatility models and therefore struggle to effectively capture long-term memory volatility (Wu et al., 2023). The GM model (Engle et al., 2013), another member of the GARCH class, addresses this limitation effectively. This model directly integrates low-frequency macroeconomic variables with high-frequency financial data without altering their frequency, preserving the most realistic and valid information in high-frequency data. Additionally, the GM model captures both the short-term and long-term components of stock market volatility.

Engle et al. (2013) point out that when examining the relationship between stock market volatility and macroeconomic activities, models that use a distinction between short-term and long-term movements outperform traditional time series volatility models in terms of forecasting performance over both the time horizon and longer time horizons. Specifically, the advent of GM introduced by Engle and Patton (2007) and Engle et al. (2013) provide new ideas for volatility modeling and forecasting by utilizing low-frequency data as the long-term component of volatility predictors. According to Engle et al. (2013), the contribution of this newly proposed method is that by including low-frequency data, the long-term component of volatility can be explained. In addition, the impact of low-frequency variables on return volatility can also be observed (Asgharian et al., 2013). The GM method was introduced to investigate the relationship between volatility and low-frequency variables, mainly macroeconomic indicators that can determine the long-term behavior of volatility. In general, GM, the core innovation of the model, is to decompose volatility into short-term volatility components and long-term volatility components, to more comprehensively capture the dynamic characteristics of market fluctuations. The short-term volatility component reflects the high-frequency fluctuations of the market in the short term (such as daily or weekly). This component is usually modeled through the GARCH process (Bollerslev, 1986). It is characterized by fast mean reversion, sensitive response to market shocks but rapid decay.

The long-term volatility component describes the trend changes of volatility on a low-frequency scale (such as monthly, quarterly or even annual), which is usually related to macroeconomic fundamentals, structural policy changes or long-term risk factors. This component is modeled through MIDAS (mixed data sampling) regression (Liu et al., 2021), allowing low-frequency macro variables (such as GDP growth rate, inflation rate, industrial production index) to be introduced into the model through weighted lag terms (such as Beta weight function). The long-term volatility component changes slowly and is more persistent, and its impact may last for months or even years (Schwert, 1989).

However, these collected low-frequency macro-variables tend to exhibit linear characteristics. Manera and Forte (2002) show that nonlinear models generally produce better forecasts with smaller forecast errors and lower bias compared to the standard GARCH specification. Guidolin et al. (2009) study the forecasting performance of linear and nonlinear models for G7 stock and bond returns. They highlighted that capturing nonlinear effects may improve forecasts. Wang et al. (2020) find that the extended nonlinear GM model performs significantly better than the traditional GM model in forecasting. Amendola et al. (2021) analyze S&P 500 and Nasdaq volatility. Their results show that the nonlinear bi-asymmetric GM model forecasts more accurately over long horizons. They also find that the expanded nonlinear GM model outperforms the traditional GM model in terms of forecasting ability. Additionally, Wu et al. (2020) analyze the performance of low-frequency economic indicators and volatility factors in predicting crude oil futures price fluctuations. They conclude that the nonlinear volatility effect model outperforms the level effect model in terms of overall estimation performance. These studies collectively underscore the superiority of nonlinear models in predicting volatility.

As machine learning and deep learning models become widely used in financial markets, they achieve remarkable results in predicting volatility. For example, Amirshahi and Lahmiri (2023) and Rayadurgam and Mangalagiri (2023) use the GARCH model as a feature extractor for deep learning models and demonstrate that the feature information extracted by the GARCH model significantly enhances the predictive ability of deep learning models. Han et al. (2024) employ a GARCH model to capture the volatility characteristics of time series, followed by data decomposition using complete ensemble empirical modal decomposition of adaptive noise (CEEMDAN), which significantly reduces data complexity. They then apply a graph convolutional network (GCN) to efficiently learn the features of the decomposed data. This model achieves higher prediction accuracy and greater stability compared to traditional methods.

However, most current research focuses on using traditional econometric models to provide effective features for machine learning or deep learning models to enhance their predictive capabilities and has not fully expanded on how to introduce the advantages of deep learning into traditional econometric models. To this end, this study aims to incorporate deep learning models into the traditional econometric GM model by extracting more complex and nonlinear deep features from macro variables through deep learning techniques and using them as low-frequency factors in the GM model. This approach not only captures the long-term trend of the market but also introduces more expressive nonlinear information into the traditional econometric model, thereby improving the accuracy of volatility forecasting.

The deep learning model chosen for this study is the KAN (Kolmogorov–Arnold Network) model, a new forecasting model recently proposed by Liu et al. (2024). It features a novel neural network structure that has the potential to replace the traditional multilayer perceptron. Linear weights are replaced with spline-based univariate functions, structured as learnable activation functions. This design not only improves the accuracy and interpretability of the networks but also enables them to obtain comparable or superior results in various tasks, such as data fitting and solving partial differential equations, with smaller network sizes. KANs have shown promise in improving the efficiency and interpretability of neural network techniques. Although no study has yet used them for volatility forecasting, they offer unique advantages. KAN models can capture the intrinsic nonlinear structure of data more efficiently by approximating complex nonlinear functions and may theoretically excel in nonlinear forecasting tasks for financial time series. This study will also explore the potential of the KAN model in volatility forecasting to further improve forecasting accuracy and the broad applicability of the model.

This study selected the US S&P 500 Index (SP 500) and Japan's Nikkei 225 Index (N225) as research objects, mainly based on their representativeness in the global financial market, differences in industry structure and comprehensive considerations of market depth.

First, as the benchmark stock index of the world's largest economy, the United States, the SP 500 covers a variety of industries such as technology, finance, and consumption, reflecting the typical characteristics of mature markets, and its volatility has a weathervane effect on global risk sentiment. The N225 represents the capital market of Japan, the most important developed economy in Asia. Its constituent stocks are centered on high-end manufacturing (such as automobiles and electronics), and are significantly affected by export trade, exchange rate fluctuations and local monetary policies (such as ETF purchases by the Bank of Japan). The difference in industry distribution between the two (the United States is dominated by technology and consumption, and Japan is good at manufacturing) provides an ideal comparison for studying volatility drivers under different economic forms.

In addition, both indices occupy a core position in the global financial system: the New York Stock Exchange where the SP500 is located and the Tokyo Stock Exchange where the N225 is located are both known for their high liquidity, large market capitalization and mature derivatives markets, ensuring the reliability of data and the effectiveness of market behavior. This choice can not only capture the common laws of developed markets but also deepen the understanding of global financial linkages through cross-market comparisons.

Existing research shows that macroeconomic variables play a key role in influencing and predicting stock market fluctuations. According to stock valuation theory, a company's stock price reflects the discounted value of its future cash flow, and changes in macroeconomic policies will lead to stock price fluctuations by affecting corporate cash flow expectations (Camilleri et al., 2019; Song et al., 2023). Based on this theoretical framework, this study selects four core macroeconomic variables: consumer price index (CPI), money supply (M2), exchange rate (ER), and economic policy uncertainty (EPU) for investigation.

In terms of inflation factors, many studies have confirmed that CPI has a significant impact on stock market fluctuations, but there are differences in the specific direction of action. Khan et al. (2014) and Okechukwu et al. (2019) find that inflation was positively correlated with stock market volatility in Nigeria and Pakistan, respectively, while Asravor and Fonu (2021) report a negative impact. Similarly, there are differences in the impact of money supply (M2): the results of Ghani et al. (2022) show that M2 is an effective volatility predictor, Cheng and Shi (2020) point out that its shocks can lead to large market fluctuations, but Wei et al. (2021) find that M2 growth may reduce industrial stock volatility by enhancing investor confidence.

Exchange rate variables are an important factor affecting stock market volatility. Chinzara (2011) found that the impact of ER exceeds that of other macroeconomic variables, and this conclusion is supported by Hajilee and Nasser (2014) and Mroua and Trabelsi (2020), whose research shows that exchange rate fluctuations have significant short- and long-term effects on stock market development.

In recent years, economic policy uncertainty (EPU) has received widespread attention. The EPU index developed by Baker et al. (2016) provides an important tool for related research. Most studies found that EPU is positively correlated with stock market volatility (Mishra & Debata, 2020; Su et al., 2019; Yu et al., 2018), but some studies, such as Li et al. (2019) and Wu et al. (2021), report a negative impact of EPU on the Chinese stock market. It is worth noting that the studies of Li et al. (2020) and Xu et al. (2021) further confirmed the practical value of EPU in predicting stock market volatility.

2. Methodology

This study aims to integrate the KAN model with the GM model. The KAN model's strengths in nonlinear representation and feature extraction will be used to extract deep features from macroeconomic variables. These features will then serve as low-frequency factors in the GM model. The KAN model excels at capturing complex nonlinear relationships, which helps extract low-frequency information critical to volatility forecasting from multidimensional macroeconomic data. The GM model combines these low-frequency features with high-frequency volatility to achieve more accurate volatility modeling and forecasting of financial time series.

During the model training process, the optimization algorithm chosen is the gradient-based BFGS (Broyden–Fletcher–Goldfarb–Shanno) algorithm, known for its high efficiency in dealing with large-scale parameter optimization problems. The following sections will detail the construction of the KAN model and the GM model, along with their specific applications in this study.

2.1 KAN model

If f is a multivariate continuous function defined on a bounded region, then it can be expressed as a finite combination of univariate continuous functions and additive binary operations. In particular, this smooth and continuous multivariate function $f(x)\colon [0,\ 1]^n \to \mathbb{R}$ can be expressed by a superposition of univariate functions of finite times.

$$f(x) = f(x_1, \ldots, x_n) = \sum_{q=1}^{2n+1} \Phi_q\left(\sum_{p=1}^{n} \varnothing_{q,p}(x_p)\right) \tag{1}$$

where $\varnothing_{q,p}\colon [0,\ 1] \to \mathbb{R}$ and $\varnothing_q\colon \mathbb{R} \to \mathbb{R}$ denote the so-called “intrinsic and extrinsic functions”, respectively. Liu et al. (2024) state that Equation (1) exhibits a two-layer nonlinear feature, and the hidden layer contains only a small number (2n + 1) terms. When dealing with the learning task of the input-output pair $\{x_i, y_i\}$, the key is to construct a function f so that all data points satisfy $y_i \approx f(x_i)$. Studies have shown that if suitable univariate functions $\varnothing_{q,p}$ and Φ_q can be determined, the problem can be effectively solved. This discovery prompted the researchers to design a neural network architecture that can explicitly parameterize Equation (1).

Given that all functions to be learned are univariate functions, the research team used B-spline curves to parameterize each one-dimensional function and optimized it by learning the coefficients of local B-spline basis functions. This formed the preliminary architecture of the KAN model, whose calculation process is clearly defined by Equation (1). It is worth noting that, unlike the traditional Kolmogorov–Arnold model, the KAN model uses a KAN layer structure with n input and n output dimensions, which is essentially a matrix form composed of one-dimensional functions.

Once a layer consisting of a linear transformation and a nonlinear function is defined, the network can be made deeper by superimposing more layers. A deep KAN layer with non-one-dimensional inputs and non-one-dimensional outputs can be represented as a matrix form consisting of one-dimensional functions.

$$\Phi = \{\varnothing_{q,p}\} \tag{2}$$

where $p = 1,2, \ldots, n_{in}$, $q = 1,2, \ldots, n_{out}$, n_{in} and n_{out} denote the number of inputs and outputs respectively, and $\varnothing_{q,p}$ has trainable parameters. Thus, the Kolmogorov–Arnold representation theorem can be a simple composition of two KAN layers. The internal function with $n_{in} = n$ and $n_{out} = 2n + 1$ constitutes one KAN layer, and the external function constitutes the other KAN layer via $n_{in} = 2n + 1$ and $n_{out} = 1$. It can be seen that the Kolmogorov–Arnold representation described in Equation (1) is essentially a combination of two KAN layers. Therefore, to achieve a deeper Kolmogorov–Arnold representation, the key is to stack more KAN layers.

The shape of KAN is denoted by $[n_0, , \ldots, n_L]$, where n_i is the number of nodes in layer i of the computational graph. (l, i) denotes the ith neuron in layer l and $x_{l,i}$ denotes the activation value of the (l, i) neuron. Between layer l and layer $l + 1$, there is $n_l n_{l+1}$ activation function, which connects (l, i) and $(l + 1, j)$ and can be defined as:

$$\varnothing_{l,j,i},\ l = 0, \ldots, L - 1,\ i = 1, \ldots, n_l,\ j = 1, \ldots, n_{l+1} \tag{3}$$

The reactivation of $\varnothing_{l,j,i}$ is $x_{l,i}$ and its post-activation is $\tilde{x}_{l,j,i} \equiv \varnothing_{l,j,i}(x_{l,i})$. The activation value of a neuron $(l + 1, j)$ can be simply expressed as the sum of all incoming posterior activations, expressed as follows:

$$x_{l+1,j} = \sum_{i=1}^{n_l} \tilde{x}_{l,j,i} = \sum_{i=1}^{n_l} \varnothing_{l,j,i}(x_{l,i}),\ j = 1, \ldots, n_{l+1} \tag{4}$$

In matrix form, it can be written as:

$$\mathrm{x}_{l+1} = \begin{pmatrix} \varnothing_{l,1,1}(\cdot) & \varnothing_{l,1,2}(\cdot) & \cdots & \varnothing_{l,1,n_l}(\cdot) \\ \varnothing_{l,2,1}(\cdot) & \varnothing_{l,2,2}(\cdot) & \cdots & \varnothing_{l,2,n_l}(\cdot) \\ \vdots & \vdots & \ddots & \vdots \\ \varnothing_{l,n_{l+1},1}(\cdot) & \varnothing_{l,n_{l+1},2}(\cdot) & \cdots & \varnothing_{l,n_{l+1},n_l}(\cdot) \end{pmatrix} \mathrm{x}_l$$

When given an input vector $x_0 \in \mathbb{R}^{n_0}$, the KAN network can be represented by a combination of L layers:

$$KAN(x) = (\Phi_{L-1} \circ \Phi_{L-2} \circ \cdots \Phi_1 \circ \Phi_0)x \tag{5}$$

Rewrite the above formula in a form similar to Equation (1), let $f(x) \equiv KAN(x)$ when the output dimension $n_L = 1$, and the specific expression is as follows:

$$f(\mathrm{x}) = \sum_{i_{L-1}=1}^{n_{L-1}} \varnothing_{L-1,i_L,i_{L-1}} \left(\sum_{i_{L-2}=1}^{n_{L-2}} \cdots \left(\sum_{i_2=1}^{n_2} \varnothing_{2,i_3,i_2} \left(\sum_{i_1=1}^{n_1} \varnothing_{1,i_3,i_2} \left(\sum_{i_0=1}^{n_0} \varnothing_{0,i_1,i_0}(x_{i_0}) \right) \right) \right) \cdots \right)$$

It is worth noting that all operations are differentiable and therefore, KANs can be trained by back-propagation. To make the KAN layer represented in Equation (4) well optimizable it is necessary to focus on three components: the residual activation function, the initialization ratio, and the update of the spline grid.

For the residual activation function, the activation function $\varnothing(x)$ can be formulated as follows:

$$\varnothing(x) = w_b b(x) + w_b spline(x) \tag{6}$$

The basis function $b(x)$ is analogous to the residual connection,

$$b(x) = silu(x) = \frac{x}{1 + e^{-x}} \tag{7}$$

$$Spline\,(x)$$

Spline(x) is parameterized as a linear combination of B-splines.

$$spline\,(x) = \sum_i c_i B_i\,(x) \tag{8}$$

where the c_i part is trainable.

For initialization scaling, each activation function is initialized to $w_s = 1$ and $spline\,(x) \approx 0$, and w_b is initialized according to the Xavier initialization. The update of the spline lattice is dynamically adjusted based on the input activations of each lattice, aiming at solving the problem that spline curves, although defined on a bounded region, may have their activation values extended from a fixed region during the training process.

2.2 GARCH-MIDAS (GM) model

The GM model utilized in this study draws its foundation from the work of Engle et al. (2013) and Engle and Rangel (2008). The characterization of volatility within the framework of the GM model can be articulated as follows

$$r_{i,t} - E_{i-1,t}\,(r_{i,t}) = \sqrt{\tau_t g_{i,t}}\,\varepsilon_{i,t},\ \ E_{i-1,t}\,(r_{i,t}) = \mu,\ \ \forall\, i = 1,\ 2\ ,\ \cdots\ ,\ N_t \tag{9}$$

$$\varepsilon_{i,t}|\psi_{i-1,t}\sim N\,(0{,}1),\qquad \sigma^2_{i,t} = \tau_i g_{i,t} \tag{10}$$

In Equation (9), the expression for volatility is decomposed into two components: the short-term volatility $g_{i,t}$, which satisfies to the GARCH (1, 1) model, and long-term volatility τ_i. $E_{i-1,t}$ denotes the conditional expectation while $\varepsilon_{i,t}$ represents the random disturbance term, assumed to follow a standard normal distribution. N_t signifies the number of days in month t. $\psi_{i-1,t}$ in Equation (10) delineates the information set pertaining to the i−1 day of the rate of return in month t.

The long-term component τ_i is delineated through the incorporation of diverse low-frequency variables, encompassing factors such as CPI, M2, ER, and EPU.

$$\log(\tau_t) = m + \textstyle\sum_{i=1}^{N}\ \theta_i \sum_{k=1}^{K_i}\ \varphi_{i,k}\,(\omega_{i,1},\ \omega_{i,2}) X_{i,t-k} \tag{11}$$

where k denotes the maximum lag order of low-frequency variables, selected by AIC and BIC information standards. N is the number of macroscopic variables. X corresponds to the macroeconomic variable. $\varphi_k\,(\omega_1,\ \omega_2)$ is the weight scheme of the Beta lag structure (Engle et al., 2013), because it is more flexible and more commonly used to accommodate various lag structures (Ghysels et al., 2007), the polynomial is shown below:

$$\varphi_k\,(\omega_1,\ \omega_2) = \frac{[k/(K+1)]^{\,\omega_1-1}[1 - k/(K+1)]^{\omega_2-1}}{\sum_{j=1}^{K}\,(j/K+1)^{\omega_1-1}[1 - j/(K+1)]^{\omega_2-1}} \tag{12}$$

Fix $\omega_1 = 1$, to ensure that the weight of the lag variable is in the form of attenuation. In other words, the closer the distance to the current period, the greater the impact on the current period (Yaya et al., 2022). The coefficient determines the attenuation speed of the impact of low-frequency data on high-frequency data. Therefore, the polynomial can be simplified as:

$$\varphi_k\,(\omega_2) = \frac{[1 - \kappa/(K+1)]^{\omega_2-1}}{\sum_{j=1}^{K}\,[1 - j/(K+1)]^{\omega_2-1}} \tag{13}$$

3. Data description and preliminary analysis

This study focuses on the stock markets of the U.S. and Japan during the period from 1 October 2009 to 31 March 2023. For the U.S., the Standard and Poor's 500 daily stock closing prices are selected, containing 3,398 observations. The Japanese daily stock closing prices are derived from the Nikkei 225, with 3,298 observations. The stock price data is sourced from Yahoo Finance (https://finance.yahoo.com). The macroeconomic variables selected include the consumer price index (CPI), money supply (M2), foreign exchange (ER), and economic policy uncertainty (EPU). For the U.S., the foreign exchange data is represented by the U.S. dollar index.

For ease of identification, EPU variables are prefixed with "U" and "J" to indicate that they originate from the U.S. and Japan, respectively. Additionally, the stock returns for these markets are calculated using logarithmic prices, with the returns denoted as SP500 and N225, respectively. The stock return used in the experiment is the log return on day i in month t, calculated as follows:

$$r_{i,t} = \ln(P_{i,t}) - \ln\ (P_{i-1,t})$$

where $P_{i,t}$ represents the price for day i in month t, $t = 1, \ldots, T$ and $i = 1, \ldots, N_t$.

Table 1 presents the descriptive statistics of stock returns and various economic variables. The results indicate that the SP500 has higher average stock returns than the N225, but its FX index is the lowest at only 0.0682. Additionally, both stock markets exhibit returns that are negatively skewed and leptokurtic, with kurtosis values exceeding three. This indicates that they do not conform to a normal distribution and are characterized by sharp peaks and thick trailing tails, shifted to the left.

The kurtosis value of UEM is less than three, and the p-value is greater than 10%, indicating no significant deviation from a normal distribution. This suggests that UEM conforms to or is close to the normal distribution. In contrast, the other macroeconomic variables deviate from the normal distribution and are shifted to the right.

Table 2 presents the results of the unit root test, the Ljung–Box Q statistic, and the ARCH test. The unit root test assesses the stationarity of the time series using the Augmented Dickey–Fuller (ADF) test, Phillips–Perron (PP) test, and Kwiatkowski–Phillips–Schmidt–Shin (KPSS) test. The results of the ADF, PP, and KPSS tests indicate that both series of stock returns are stable.

Before building the volatility forecasting model, a diagnostic test of the residuals is necessary to detect autocorrelation and heteroskedasticity (i.e., the autocorrelation and variance constancy of the error term). McLeod and Li (1983) proposed a diagnostic test for the white noise properties of residuals, the Ljung–Box Q statistic test (Ljung & Box, 1979).

In Table 2, the results of the Ljung–Box Q statistic test for the autocorrelation of the stock market return series show that the SP500 return series exhibits significant p-values under this test. This suggests

Table 1. Descriptive statistics.

	Mean	Median	Max	Min	Std. Dev	Skewness	Kurtosis	*P*(JB)
SP500	0.0173	0.0280	3.8949	−5.5439	0.4870	−0.7220	15.8770	0.0000
N225	0.0134	0.0282	3.3934	−4.8439	0.5718	−0.3915	7.8725	0.0000
				Macroeconomic data				
UCPI	2.4833	1.9000	9.1000	−0.2000	2.0632	1.6236	5.0381	0.0000
UM2	7.3846	6.1350	26.6400	−3.9200	5.4475	1.8315	6.6625	0.0000
UEM	0.0682	0.0787	1.5751	−1.2026	0.5335	0.1675	2.8300	0.6210
UEPU	141.7790	136.3837	350.4598	71.2621	45.8044	1.4219	6.0948	0.0000
JCPI	0.5414	0.3000	4.3000	−2.5000	1.2729	0.9683	3.7478	0.0000
JM2	3.6276	3.1950	9.6100	2.1200	1.6005	2.5352	8.9617	0.0000
JEM	0.1023	0.0485	3.2048	−2.3588	0.9318	0.6147	3.9932	0.0002
JEPU	115.1044	110.6827	230.2788	63.6454	29.8555	1.2813	5.2294	0.0000

Table 2. Stationary testing and heteroskedastic test.

	ADF	PP	KPSS	Ljung–Box Q-statistic (36)	ARCH
SP500	−19.5543*** (0.0000)	−66.3585*** (0.0001)	0.0301	306.2200*** (0.0000)	882.6692*** (0.0000)
N225	−58.7696*** (0.0001)	−58.8264*** (0.0001)	0.0433	38.9950 (0.3370)	290.6381*** (0.0000)

Notes: The values in this table are the t-statistics for the stationary test. *** Indicate rejections of the null hypothesis at the 1% significance level.

significant autocorrelation in the residual series of these markets, leading to the rejection of the null hypothesis of no autocorrelation. This result indicates that the volatility of current returns is significantly influenced by the volatility of the previous period. However, this autocorrelation feature can be effectively addressed by the GARCH model. Additionally, the results of the ARCH test indicate that both series reject the null hypothesis at the 1% level of significance. This finding suggests the presence of significant heteroskedasticity effects in these stock markets and supports the applicability of GARCH-like models for capturing the volatility characteristics of these markets.

4. Empirical results

4.1 In-sample result

Tables 3 and 4 present the in-sample results for the two stock markets under different models. These results are estimated based on the GM model with the unconditional mean return (μ), the ARCH term (α), the GARCH term (β), the MIDAS slope coefficients (θ), the adjusted β polynomial weights (w), and the long-run constant term (m).

In the GM model, the MIDAS slope coefficient is a key parameter, reflecting the ability of macroeconomic variables to predict the volatility of stock returns. The adjusted β polynomial weights are all greater than 1, indicating that the influence of macro variables diminishes as the time interval increases. Additionally, the ARCH (α) and GARCH (β) terms are significantly positive (at the 1% level) across all models, suggesting that the short-term component contributes significantly to the intraday volatility of stock returns. Notably, $\alpha + \beta$ is close to but less than 1, indicating significant volatility persistence and mean reversion in stock market returns.

The MIDAS slope coefficient represents the sum of the actual volatility of each variable weighted by the rolling window, capturing the effect of low-frequency macro variables on stock volatility. The impact of low-frequency factors varies between stock markets. For instance, CPI has a significant positive effect on SP500 volatility, while EPU has a weaker positive effect. In the Japanese market, CPI has a significant negative effect on N225 volatility, whereas exchange rate changes exhibit a stronger positive effect on N225 volatility. Furthermore, although M2 shows a negative effect on equity volatility, it is not statistically significant.

4.2 Out-of-sample result

Market participants are more interested in a model's ability to predict future stock volatility rather than just its in-sample performance (Ma et al., 2019b; Wang et al., 2020; Yu & Huang, 2021). Since most investors aim to uncover new investment opportunities from historical market information, models with higher efficiency are required to help mine this information effectively. Therefore, this section focuses on analyzing whether models with additive outliers can enhance predictive ability. All models in this study employ fixed-window forecasting. The stock return data is divided into two subgroups for forecasting: the in-sample group accounts for 80% of the total sample, while the out-of-sample group accounts for the remaining 20%, corresponding to 660 forecasting periods.

This study determined the key hyperparameter range of the KAN-GARCH-MIDAS model through systematic parameter optimization. Based on the criterion of minimizing the log-likelihood function value (llh), empirical analysis shows that the optimal value ranges of the shape parameter (width) of the polynomial in KAN, the high-frequency data aggregation granularity (grid), and the order of the polynomial in KAN are all 1–5. When the values of these parameters exceed 5, the model will show obvious overfitting, which is manifested by a significant increase in the log-likelihood function value (llh) and a decrease in the model fitting effect. Therefore, the parameter combinations finally selected in this study are all within a reasonable range of 1–5 to ensure that the model avoids overfitting problems while maintaining good fitting performance. When the selected parameters are greater than 5, the loss function value of the out-of-sample prediction increases significantly and the prediction performance decreases. The selection of all parameters strictly follows the principle of minimizing the llh value, thereby ensuring the optimal performance of the model.

Table 3. In-sample estimation results, SP500.

Model	μ	α	β	m	θ_{CPI}	θ_{M2}	θ_{ER}	θ_{EPU}	ω_{CPI}	ω_{M2}	ω_{EM}	ω_{EPU}	LLF/AIC	LLF/BIC
GARCH	0.0335*** (0.0057)	0.1782*** (0.0231)	0.7966*** (0.0215)	−1.2953*** (0.3498)	/	/	/	/	/	/	/	/	3199.3480	3223.8810
GM-CPI	0.0340*** (0.0059)	0.1994*** (0.0290)	0.7577*** (0.0278)	−2.0173*** (0.3359)	0.2313** (0.0916)	/	/	/	1.7506 (2.6473)				2579.0580	2614.9280
GM-M2	0.0342*** (0.0060)	0.2028*** (0.0295)	0.7550*** (0.0286)	−2.1731*** (0.4468)	/	0.0820* (0.0447)	/	/	/	1.0000 (0.8623)	/	/	2377.0590	2412.6680
GM-ER	0.0348*** (0.0059)	0.2068*** (0.0314)	0.7677*** (0.0274)	−1.2215** (0.0373)	/	/	0.2448 (0.6468)	/	/	/	3.3225* (1.7847)	/	2539.6230	2575.4500
GM-EPU	0.0336*** (0.0060)	0.1987*** (0.0278)	0.7567*** (0.0276)	−2.3952*** (0.4347)	/	/	/	0.0060** (0.0026)	/	/	/	8.5864 (7.1960)	2363.9460	2399.5080
GM-CPI + M2	0.0334*** (0.0059)	0.1941*** (0.0283)	0.7404*** (0.0298)	−2.8549*** (0.3429)	0.4055*** (0.1356)	0.0394** (0.0168)	/	/	1.1245 (0.7688)	155.9042*** (28.5323)	/	/	2346.9990	2394.4140
GM-CPI + ER	0.0339*** (0.0059)	0.1985*** (0.0289)	0.7462*** (0.0304)	−2.1634*** (0.2729)	0.1610*** (0.0451)	/	1.1821* (0.7072)	/	1.0000 (4.6403)	/	2.6792*** (0.7768)	/	2383.3860	2430.9790
GM-CPI + EPU	0.0332*** (0.0059)	0.1970*** (0.0282)	0.7340*** (0.0295)	−2.8267*** (0.4187)	0.1869*** (0.0518)	/	/	0.0051* (0.0028)	1.0000 (0.0028)	/	/	12.2733* (6.5307)	2353.7260	2401.1420
GM-M2 + ER	0.0343*** (0.0059)	0.2033*** (0.0298)	0.7412*** (0.0291)	−2.5892*** (0.3869)	/	0.1057*** (0.0321)	1.2764** (0.6019)	/	/	1.0000* (0.5384)	1.0000** (0.4232)	/	2353.3560	2400.7710
GM-M2 + EPU	0.0346*** (0.0060)	0.2126*** (0.0306)	0.7382*** (0.0294)	−2.7674*** (0.4484)	/	0.0697*** (0.0187)	/	0.0049* (0.0026)	/	1.0000** (0.4525)	/	2.0084 (1.4927)	2359.5160	2406.9310
GM-ER + EPU	0.0339*** (0.0059)	0.2020*** (0.0292)	0.7353*** (0.0301)	−3.5522*** (0.7768)	/	/	1.9730* (1.1017)	0.0122** (0.0048)	/	/	2.9201** (1.4435)	1.4388 (2.7845)	2356.4350	2403.8510
GM-CPI + M2 + ER	0.0336*** (0.0058)	0.1946*** (0.0279)	0.7177*** (0.0307)	−3.2714*** (0.3408)	0.3900*** (0.1070)	0.0611*** (0.0176)	1.9011** (0.7949)	/	1.4602** (0.7436)	66.5571*** (11.0078)	2.8973** (1.1821)	/	2334.8290	2394.0980
GM-CPI + M2 + EPU	0.0332*** (0.0059)	0.1899*** (0.0277)	0.7457*** (0.0293)	−2.8746*** (0.4319)	0.4018*** (0.1417)	0.0380* (0.0231)	/	0.0002 (0.0036)	1.1108 (0.7928)	16.2937*** (2.4237)	/	6.0697* (3.5262)	2351.0380	2410.3080
Model	μ	α	β	m	θ_{CPI}	θ_{M2}	θ_{ER}	θ_{EPU}	ω_{CPI}	ω_{M2}	ω_{EM}	ω_{EPU}	LLF/AIC	LLF/BIC
GM-CPI + ER + EPU	0.0333*** (0.0059)	0.1948*** (0.0281)	0.7229*** (0.0306)	−3.4272*** (0.4457)	0.1408*** (0.0370)	/	1.8892*** (0.6957)	0.0082*** (0.0028)	8.2663 (6.3371)	/	1.3652*** (0.5177)	3.9439 (2.6349)	2341.9390	2401.2090
GM-M2 + ER + EPU	0.0340*** (0.0059)	0.1867*** (0.0271)	0.7412*** (0.0281)	−3.4047*** (0.5101)	/	0.0841** (0.0359)	1.8015*** (0.6486)	0.0059** (0.0028)	/	1.0000 (0.6517)	1.3333*** (0.6517)	6.1744** (2.7528)	2344.4370	2403.7070
GM-CPI + M2 + ER + EPU	0.0336*** (0.0059)	0.1974*** (0.0284)	0.7286** (0.0303)	−3.4047*** (0.4441)	0.0681* (0.0401)	0.0423** (0.0169)	1.8553** (0.7621)	0.0072*** (0.0027)	1.0003 (17.1257)	1.0000 (0.6918)	2.5506*** (0.8469)	9.6401** (3.7427)	2352.4840	2423.607

Notes: Standard errors in parentheses. * Indicate rejections of the null hypothesis at the 10% significance level.
** Indicate rejections of the null hypothesis at the 5% significance level.
*** Indicate rejections of the null hypothesis at the 1% significance level. The numbers in parentheses are the *p*-values of the tests.

Table 4. In-sample estimation results, N225.

Model	μ	α	β	m	θ_{CPI}	θ_{M2}	θ_{ER}	θ_{EPU}	ω_{CPI}	ω_{M2}	ω_{EM}	ω_{EPU}	LLF/AIC	LLF/BIC
GARCH	0.0276*** (0.0086)	0.1259*** (0.0000)	0.8295*** (0.0298)	−1.0662*** (0.1555)	/	/	/	/	/	/	/	/	5129.2680	5153.6720
GM-CPI	0.0274*** (0.0087)	0.1251*** (0.0225)	0.8312*** (0.0307)	−0.9991*** (0.1734)	−0.1028* (0.0602)	/	/	/	1.0000 (1.8878)	/	/	/	4905.6960	4942.0380
GM-M2	0.0286*** (0.0093)	0.1059*** (0.0226)	0.8609*** (0.0329)	−1.0821** (0.5054)	/	−0.0022 (0.1278)	/	/	/	8.0017 (0.0128)	/	/	4331.9200	4367.6040
GM-ER	0.0271*** (0.0094)	0.1066*** (0.0246)	0.8554*** (0.0377)	−1.2172*** (0.1808)	/	/	0.6758* (0.3670)	/	/	/	2.8016 (4.4928)	/	4116.6280	4151.9970
GM-EPU	0.0281*** (0.0091)	0.1272*** (0.0244)	0.8321*** (0.0347)	−0.2624 (0.4332)	/	/	/	−0.0067-** (0.0032)	/	/	/	1.0000 (0.7561)	4570.2890	4606.2350
GM-CPI + M2	0.0271*** (0.0095)	0.1073*** (0.0225)	0.8554*** (0.0331)	−0.9947*** (0.2752)	−0.0649* (0.0378)	−0.0193 (0.7205)	/	/	1.0000 (3.8371)	16.2014 (16.290-8)	/	/	4153.4030	4200.6230
GM-CPI + ER	0.0290*** (0.0091)	0.1104*** (0.0215)	0.8235*** (0.0365)	−1.1737*** (0.1290)	−0.3915*-** (0.1001)	/	1.8221*** (0.4275)	/	1.5384* (0.8152)	/	1.6286**-* (0.2414)	/	4097.4550	4144.6130
GM-CPI + EPU	0.0271*** (0.0095)	0.1119*** (0.0244)	0.8465*** (0.0370)	1.0232 (1.1851)	−0.2523* (0.1301)	/	/	−0.0173* (0.0096)	1.5087* (0.8623)	/	/	2.0458*** (0.6408)	4120.3070	4167.4650
GM-M2 + ER	0.0275*** (0.0093)	0.1065*** (0.0242)	0.8563*** (0.0364)	−1.0207 (0.3344)	/	−0.0467 (0.3344)	0.4160* (0.2126)	/	/	1.0000 (9.2505)	3.2334* (1.6711)	/	4117.2890	4164.4470
GM-M2 + EPU	0.0285*** (0.0091)	0.1300*** (0.0241)	0.8236*** (0.0334)	−0.9358*** (0.2689)	/	−0.0050 (0.0510)	−0.0011* (0.0006)	/	/	8.2119 (0.4814)	/	1.0000 (1.2463)	4598.5430	4646.5220
GM-ER + EPU	0.0286*** (0.0091)	0.0912*** (0.0219)	0.8821*** (0.0320)	−0.3021 (0.5611)	/	/	0.3358** (0.1674)	−0.0074* (0.0043)	/	/	10.8185*-** (4.1553)	1.0036 (0.8555)	4245.0340	4292.4930
GM-CPI + M2 + ER	0.0290*** (0.0091)	0.1117*** (0.0218)	0.8180*** (0.0380)	−0.9207*** (0.1904)	−0.4315*-** (0.0972)	−0.0617* (0.0335)	1.8796*** (0.4115)	/	1.3840* (0.8174)	1.0001 (7.3591)	1.5971**-* (0.2255)	/	4098.4030	4157.3500
Model	μ	α	β	m	θ_{CPI}	θ_{M2}	θ_{ER}	θ_{EPU}	ω_{CPI}	ω_{M2}	ω_{EM}	ω_{EPU}	LLF/AIC	LLF/BIC
GM-CPI + M2 + EPU	0.0271*** (0.0095)	0.1010*** (0.0221)	0.8581*** (0.0341)	0.9062 (1.0166)	−0.2638* (0.1368)	−0.0010 (0.0022)	/	−0.0166* (0.0086)	1.2910 (0.9394)	5.9881 (34.736-5)	/	1.0000 (0.8832)	4117.8510	4176.7980
GM-CPI + ER + EPU	0.0288*** (0.0091)	0.1089*** (0.0218)	0.8260*** (0.0356)	0.0176 (0.3841)	−0.4561*-** (0.0995)	/	1.5950*** (0.4471)	−0.0099-*** (0.0031)	1.3883** (0.6626)	/	1.6282**-* (0.3091)	1.0000** (0.4228)	4095.2440	4154.1910
GM-M2 + ER + EPU	0.0292*** (0.0088)	0.1312*** (0.0247)	0.8202*** (0.0344)	−1.0328*** (0.2636)	/	-0.0104 (0.0537)	0.3419* (0.1784)	−0.0005-** (0.0003)	/	3.3107 (8.1484)	6.7271**-* (2.5568)	1.0000 (1.3218)	4592.6450	4652.6180
GM-CPI + M2 + ER + EPU	0.0288*** (0.0091)	0.1039*** (0.0203)	0.8273*** (0.0356)	0.3554 (0.5337)	−0.5090*-** (0.1125)	−0.0714 (0.6319)	1.6910*** (0.4257)	−0.0105-*** (0.0034)	1.5755** (0.6319)	2.7855 (4.5785)	1.6031**-* (0.2972)	1.0000** (0.4017)	4096.5220	4167.2590

Notes: Standard errors in parentheses. * Indicate rejections of the null hypothesis at the 10% significance level.
** Indicate rejections of the null hypothesis at the 5% significance level.
*** Indicate rejections of the null hypothesis at the 1% significance level. The numbers in parentheses are the *p*-values of the tests.

Kou et al. (2021) state that using multiple criteria makes the analysis more effective. Therefore, three loss functions are selected in this study to evaluate the predictive performance of the models: mean absolute error (MAE), root mean squared error (RMSE), and median absolute error (MedAE). RMSE, the square root of the mean of the squared prediction errors, penalizes large errors more severely due to the squared term magnifying differences. Brooks (1998) states that RMSE is the most preferred accuracy criterion for evaluating prediction models. However, this criterion, which employs a quadratic loss function, may lead to misleading conclusions in the presence of outliers (Liu et al., 2020). MAE is therefore necessary as it evaluates model performance without being overly influenced by outliers, making it more stable in their presence (Park, 2002). This loss function is also frequently used to assess the predictive accuracy of competing models (e.g., Lahmiri (2020); Sadorsky (2005)). MedAE, the median absolute error, differs from the other two loss functions by using the median instead of the mean. This approach ensures robust estimates of the central tendency and minimizes the influence of outliers (Liu et al., 2020). Even when outliers are present, MedAE remains largely unaffected. The expressions of the selected loss functions are provided below:

$$MAE = \frac{1}{n}\sum_{t=1}^{n}|\sigma_t - \hat{\sigma}_t|,$$

$$RMSE = \sqrt{\frac{1}{n}\sum_{t=1}^{n}(\sigma_t - \hat{\sigma}_t)^2},$$

$$MedAE = Median|\sigma_t - \hat{\sigma}_t|,$$

Table 5 presents the out-of-sample forecasts of SP500 and N225 volatility by different models, offering a comprehensive view of each model's forecasting performance. The "mean value" column represents the average of MAE, RMSE, and MedAE, with the top five values showing lower forecast errors bolded. Traditional GARCH models and GARCH-MIDAS (GM) models based on a single macroeconomic

Table 5. Out-of-sample prediction results.

	SP500				N225			
Model	MAE	RMSE	MedAE	Mean value	MAE	RMSE	MedAE	Mean value
GARCH	0.2743	0.4835	0.1516	0.3031	0.2784	0.3976	0.2159	0.2973
GM-CPI	0.2682	0.4856	0.1407	0.2982	0.2783	0.3975	0.2156	0.2971
GM-M2	0.2708	0.4842	0.1462	0.3004	0.2579	0.3973	0.1749	0.2767
GM-ER	0.2721	0.4831	0.1493	0.3015	0.2840	0.3999	0.2213	0.3017
GM-EPU	0.2735	0.4837	0.1503	0.3025	0.2775	0.3975	0.2137	0.2962
GM-CPI + M2	0.2665	0.4862	0.1362	0.2963	0.2542	0.3978	0.1688	0.2736
GM-CPI + ER	0.2677	0.4856	0.1399	0.2977	0.2832	0.3975	0.2313	0.3040
GM-CPI + EPU	0.2684	0.4856	0.1397	0.2979	0.2762	0.3975	0.2135	0.2957
GM-M2 + ER	0.2702	0.4838	0.1453	0.2998	0.2562	0.3970	0.1711	0.2748
GM-M2 + EPU	0.2715	0.4846	0.1494	0.3018	0.2629	0.3971	0.1880	0.2827
GM-ER + EPU	0.2726	0.4827	0.1508	0.3020	0.2889	0.4025	0.2243	0.3052
GM-CPI + M2 + ER	0.2665	0.4865	0.1403	0.2978	0.2684	0.3974	0.1996	0.2885
GM-CPI + M2 + EPU	0.2672	0.4856	0.1411	0.2980	0.2482	0.3977	0.1564	0.2674
GM-CPI + ER + EPU	0.2679	0.4853	0.1411	0.2981	0.2829	0.3971	0.2265	0.3022
GM-M2 + ER + EPU	0.2686	0.4831	0.1435	0.2984	0.2720	0.3994	0.2025	0.2913
GM-CPI + M2 + ER + EPU	0.2649	0.4863	0.1365	0.2959	0.2675	0.3966	0.1948	0.2863
KAN-GM-CPI	0.2606	0.4856	0.1286	0.2916	0.2510	0.3935	0.1621	0.2689
KAN-GM-M2	0.2657	0.4782	0.1452	0.2964	0.2422	0.4003	0.1481	0.2635
KAN-GM-ER	0.2611	0.4868	0.1324	0.2934	0.2832	0.3990	0.2218	0.3013
KAN-GM-EPU	0.2668	0.4821	0.1404	0.2964	0.2540	0.3955	0.1675	0.2723
KAN-GM-CPI + M2	0.2647	0.4823	0.1433	0.2968	0.2458	0.3971	0.1539	0.2656
KAN-GM-CPI + ER	0.2647	0.4837	0.1374	0.2953	0.2766	0.3960	0.2136	0.2954
KAN-GM-CPI + EPU	0.2592	0.4791	0.1340	0.2908	0.2739	0.3944	0.2101	0.2928
KAN-GM-M2 + ER	0.2593	0.4756	0.1410	0.2920	0.2544	0.3967	0.1685	0.2732
KAN-GM-M2 + EPU	0.2532	0.4738	0.1334	0.2868	0.2530	0.3970	0.1637	0.2712
KAN-GM-ER + EPU	0.2555	0.4751	0.1372	0.2893	0.2844	0.3973	0.2288	0.3035
KAN-GM-CPI + M2 + ER	0.2602	0.4858	0.1281	0.2914	0.2642	0.3964	0.1945	0.2850
KAN-GM-CPI + M2 + EPU	0.2602	0.4811	0.1339	0.2917	0.2481	0.3967	0.1600	0.2683
KAN-GM-CPI + ER + EPU	0.2643	0.4827	0.1405	0.2958	0.2798	0.3963	0.2220	0.2994
KAN-GM-M2 + ER + EPU	0.2673	0.4826	0.1416	0.2972	0.2517	0.3977	0.1641	0.2712
KAN-GM-CPI + M2 + ER + EPU	0.2586	0.4823	0.1328	0.2912	0.2579	0.3960	0.1769	0.2769

variable demonstrate limited overall predictive power. However, multivariate GM models (e.g., GM-CPI + M2 + EPU) exhibit notable advantages in capturing volatility. For instance, the MAEs of this model are 0.2649 and 0.2482 for SP500 and N225, respectively, outperforming univariate GM models.

The introduction of deep learning techniques further enhances forecasting performance. The GARCH-MIDAS (KAN-GM) model, which leverages the Kolmogorov–Arnold network (KAN), significantly outperforms the traditional GM model across most indicators. For example, in predicting SP500, the MAE of the KAN-GM-M2 + EPU model is 0.2532, considerably lower than the GARCH model's 0.2743 and the GM-CPI model's 0.2682. Similarly, in predicting N225, the KAN-GM-M2 + EPU model achieves an MAE of 0.2481, outperforming traditional models. The KAN-GM model also demonstrates stronger robustness in MedAE. For instance, the MedAE of KAN-GM-M2 + EPU for SP500 is 0.1334, significantly lower than the GARCH model's 0.1516, highlighting its stability in handling outliers. While RMSE exhibits smaller fluctuations, the KAN-GM model still achieves lower mean square error across multiple combinations, further validating its effectiveness.

Additionally, the combination of low-frequency variables significantly affects the model's predictive performance. In the GM model, the MAE of GM-CPI + M2 + EPU is 0.2672, slightly outperforming the univariate GM-CPI (0.2682) and GM-M2 (0.2708). This trend is even more pronounced in the KAN-GM models. For instance, the MAE of KAN-GM-M2 + EPU is 0.2532, substantially better than the univariate KAN-GM-M2 model's 0.2657. Furthermore, all KAN-GM models consistently outperform their GM counterparts when incorporating the same low-frequency factors. This highlights that multifactor combinations of low-frequency variables provide more predictive information and that the KAN models excel in extracting deeper features from this information.

Overall, the results of the three loss functions consistently show that the GM model incorporating KAN has significant advantages in terms of prediction accuracy and stability, and the prediction errors are generally lower than those of other competing models, showing good bias control, especially when integrating multiple low-frequency variables, which further enhances the predictive ability of the model. This suggests that the ability of KAN to extract the deeper features of low-frequency variables is of great significance in improving the prediction of stock market volatility.

Figures 1 and 2 compare the actual volatility (black solid line) with the predicted volatility of different models. The green line represents the prediction results of the GARCH model, the red line represents the KAN-GM model, and the blue line represents the GM model. As shown in Figure 1, the KAN-GM model closely fits the actual volatility in most periods, particularly during low and medium volatility stages,

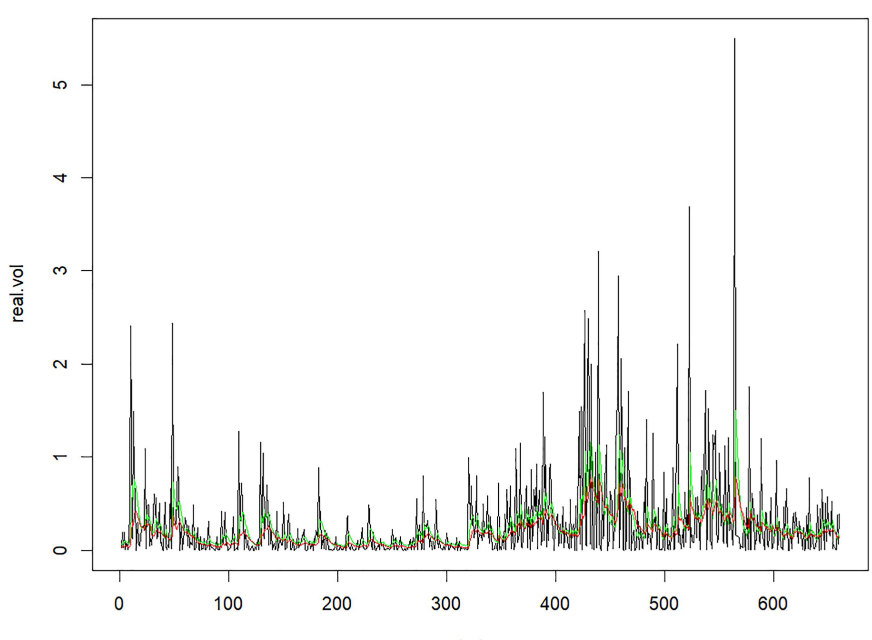

Figure 1. Forecasting performance of GARCH and KAN-GM models.

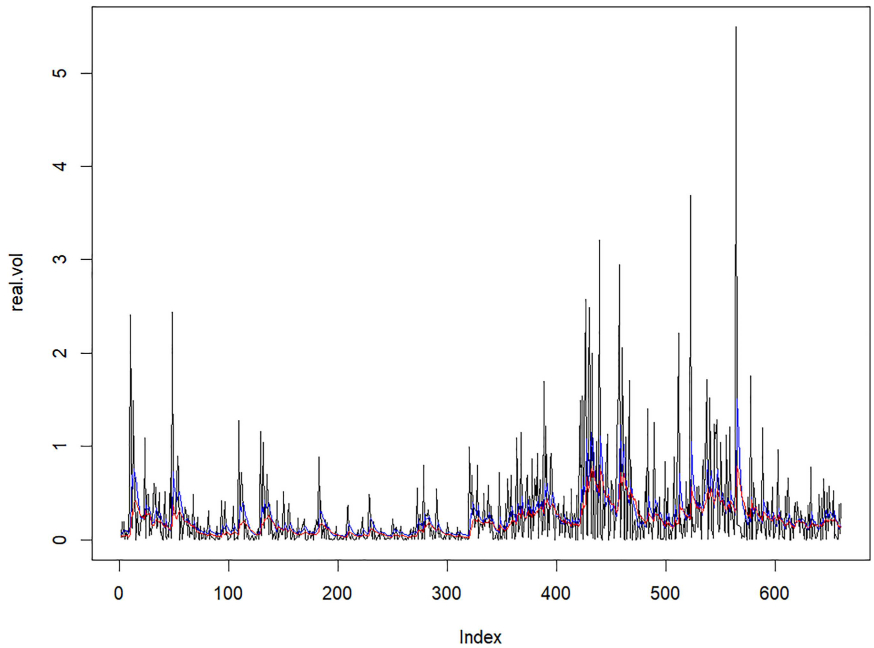

Figure 2. Forecasting performance of GM and KAN-GM models.

demonstrating significantly better prediction accuracy than the GARCH model. In contrast, the GARCH model performs relatively poorly during high-volatility periods, especially near volatility peaks, where prediction bias is substantial. This highlights the KAN-GM model's strength in capturing complex and dynamically changing volatility patterns.

Figure 2 further compares the forecasting performance of the KAN-GM model with the GM model. The results show that the KAN-GM model surpasses the GM model in overall forecasting performance, especially in accurately capturing volatility peaks during high-volatility periods, demonstrating greater flexibility. Additionally, the KAN-GM model aligns more closely with actual volatility during low-volatility periods, whereas the GM model exhibits noticeable lag or underestimation in certain periods. These findings reinforce that integrating the KAN model to extract deep features significantly enhances the KAN-GM model's prediction accuracy and robustness, offering a powerful tool for modeling and forecasting complex volatility patterns.

4.3 MCS test

This study uses the model confidence set (MCS) test (Hansen et al., 2011) to systematically evaluate the accuracy of exchange rate fluctuation forecasts. This method has the following advantages: first, there is no need to set a benchmark model when comparing model accuracy, and the operation is simple and efficient; second, it can construct a set of optimal models and retain models with equivalent predictive ability at a given confidence level (that is, the null hypothesis of equal predictive ability is not rejected). For this reason, the MCS test is widely used in model prediction performance evaluation (Ma et al., 2019a).

Specifically, this study refers to the method of Hansen et al. (2011) and uses the following test statistics:

$$T_{max,M} = max_{i \in M} \ |\bar{d}_{i.}| / \sqrt{\hat{var}(\bar{d}_{i.})}$$

where:

(1) $\bar{d}_{i.} = (m-1)^{-1} \sum_{i \in M} \bar{d}_{ij}$ represents the average loss difference of model i relative to other models in the set M.

(2) $\bar{d}_{ij}$c measures the average loss difference between models i and j.

(3) $\hat{\text{var}}(\bar{d}_{i.})$ is the bootstrap variance estimate of $\text{var}(\bar{d}_{i.})$.

The MCS test determines whether each model belongs to the optimal model set $M^*_{1-\alpha}$ by calculating the p-value (denoted as $\hat{p}_i^*$) of each model. Model i will be retained in the optimal model set with a confidence level of 1-α if and only if $\hat{p}_i^* \geq \alpha$.

This study systematically evaluates the performance of forecasting models through the MCS test. In Table 6, the results show significant model differentiation characteristics. Empirical analysis shows that KAN macroeconomic combination models show excellent forecasting ability: in SP500 forecast, KAN-GM-M2 + EPU and KAN-GM-CPI + M2 + ER + EPU models (Rank_M = 1.000) are stably selected into the optimal model set by comprehensive consideration of monetary policy and uncertainty factors; and in Nikkei 225 forecast, KAN-GM-M2 single factor model (Rank_M = 1.000) also performs well, showing its special applicability to the Japanese market. In contrast, GARCH-MIDAS models are almost all eliminated (marked with "/"). This result is highly consistent with the evaluation conclusion based on loss functions such as MAE, RMSE and MedAE, indicating that traditional volatility models have essential limitations in capturing stock market dynamics. The research findings not only confirm the importance of macro-economic fundamentals in stock market forecasting but also provide a clear empirical basis for model selection.

4.4 Model robustness test results before and after the COVID-19 epidemic

This study uses sample data from October 2009 to March 2023, and based on the exogenous shock of the COVID-19 epidemic, divides the sample into two sub-samples before the epidemic (October 2009–December 2019) and after the epidemic (January 2020–March 2023) for robustness testing. This division helps to evaluate the stability of the model under major external shocks.

Tables 7 and 8 present the empirical results of different volatility prediction models during the epidemic period and after the epidemic, respectively. By systematically comparing the performance of each model in key indicators such as MAE, RMSE, MedAE and mean error, the study found that: First, the KAN-GM model constructed in this study showed significant prediction advantages in both periods, and its various

Table 6. MCS test results of each model for predicting the volatility of SP500 and N225 indices.

	SP500		N225	
	$T_{\max,M}$	Rank_M	$T_{\max,M}$	Rank_M
GARCH	/	/	/	/
GM-CPI	/	/	/	/
GM-M2	/	/	/	/
GM-ER	/	/	/	/
GM-EPU	/	/	/	/
GM-CPI + M2	/	/	/	/
GM-CPI + ER	/	/	/	/
GM-CPI + EPU	/	/	/	/
GM-M2 + ER	/	/	/	/
GM-M2 + EPU	/	/	/	/
GM-ER + EPU	/	/	/	/
GM-CPI + M2 + ER	/	/	/	/
GM-CPI + M2 + EPU	/	/	4.0000	0.9510
GM-CPI + ER + EPU	/	/	/	/
GM-M2 + ER + EPU	/	/	/	/
GM-CPI + M2 + ER + EPU	/	/	/	/
KAN-GM-CPI	5.0000	0.5006	/	/
KAN-GM-M2	/	/	1.0000	1.0000
KAN-GM-ER	6.0000	0.4130	/	/
KAN-GM-EPU	/	/	5.0000	0.5500
KAN-GM-CPI + M2	/	/	2.0000	1.0000
KAN-GM-CPI + ER	/	/	/	/
KAN-GM-CPI + EPU	4.0000	0.9616	/	/
KAN-GM-M2 + ER	3.0000	0.9852	/	/
KAN-GM-M2 + EPU	1.0000	1.0000	/	/
KAN-GM-ER + EPU	/	/	/	/
KAN-GM-CPI + M2 + ER	/	/	/	/
KAN-GM-CPI + M2 + EPU	7.0000	0.3908	3.0000	0.9990
KAN-GM-CPI + ER + EPU	/	/	/	/
KAN-GM-M2 + ER + EPU	/	/	6.0000	0.2154
KAN-GM-CPI + M2 + ER + EPU	2.0000	1.0000	/	/

Table 7. The performance of volatility forecasting models in the pre-pandemic period.

	SP500				N225			
Model	MAE	RMSE	MedAE	Mean value	MAE	RMSE	MedAE	Mean value
GARCH	0.5921	1.0806	0.2969	0.6565	0.9140	1.3352	0.6764	0.9752
GM-CPI	0.5859	1.0819	0.2784	0.6488	0.9102	1.3322	0.6707	0.9710
GM-M2	0.5950	1.0805	0.3088	0.6615	0.9613	1.3646	0.7616	1.0292
GM-ER	0.5912	1.0805	0.2965	0.6561	0.8857	1.3105	0.6447	0.9470
GM-EPU	0.5870	1.0752	0.2921	0.6514	0.9107	1.3340	0.6926	0.9791
GM-CPI + M2	0.5875	1.0834	0.2896	0.6535	0.9645	1.3669	0.7572	1.0295
GM-CPI + ER	0.5837	1.0797	0.2750	0.6461	0.8746	1.3028	0.6367	0.9380
GM-CPI + EPU	0.5806	1.0764	0.2680	0.6417	0.9117	1.3302	0.7016	0.9812
GM-M2 + ER	0.5931	1.0743	0.3029	0.6568	0.9240	1.3279	0.7012	0.9844
GM-M2 + EPU	0.5927	1.0810	0.2913	0.6550	0.9538	1.3617	0.7543	1.0233
GM-ER + EPU	0.5885	1.0795	0.2853	0.6511	0.8805	1.3062	0.6426	0.9431
GM-CPI + M2 + ER	0.5877	1.0871	0.2810	0.6519	0.9179	1.3241	0.6837	0.9752
GM-CPI + M2 + EPU	0.5884	1.0901	0.2716	0.6500	0.9661	1.3692	0.7629	1.0327
GM-CPI + ER + EPU	0.5845	1.0937	0.2607	0.6463	0.8730	1.3013	0.6312	0.9352
GM-M2 + ER + EPU	0.5899	1.0871	0.2891	0.6554	0.9197	1.3261	0.6946	0.9802
GM-CPI + M2 + ER + EPU	0.5897	1.0956	0.2682	0.6512	0.9129	1.3197	0.6834	0.9720
KAN-GM-CPI	0.1748	0.3763	0.0711	0.2074	0.2371	0.4730	0.1392	0.2831
KAN-GM-M2	0.1744	0.3774	0.0768	0.2095	0.2628	0.4741	0.1790	0.3053
KAN-GM-ER	0.1903	0.3758	0.1051	0.2237	0.2412	0.4784	0.1351	0.2849
KAN-GM-EPU	0.1791	0.3760	0.0918	0.2156	0.2631	0.4766	0.1825	0.3074
KAN-GM-CPI + M2	0.1713	0.3757	0.0739	0.2069	0.2664	0.4716	0.1910	0.3097
KAN-GM-CPI + ER	0.1691	0.3758	0.0706	0.2052	0.2481	0.4867	0.1418	0.2922
KAN-GM-CPI + EPU	0.1637	0.3763	0.0648	0.2016	0.2440	0.4729	0.1544	0.2904
KAN-GM-M2 + ER	0.1715	0.3766	0.0717	0.2066	0.2720	0.4875	0.1754	0.3116
KAN-GM-M2 + EPU	0.1648	0.3786	0.0689	0.2041	0.2931	0.4943	0.2056	0.3310
KAN-GM-ER + EPU	0.1803	0.3755	0.0880	0.2146	0.2513	0.4807	0.1527	0.2949
KAN-GM-CPI + M2 + ER	0.1618	0.3770	0.0639	0.2009	0.2734	0.4756	0.2114	0.3202
KAN-GM-CPI + M2 + EPU	0.1629	0.3746	0.0646	0.2007	0.2944	0.5321	0.1793	0.3353
KAN-GM-CPI + ER + EPU	0.1682	0.3757	0.0763	0.2067	0.2421	0.4760	0.1398	0.2860
KAN-GM-M2 + ER + EPU	0.1648	0.3828	0.0723	0.2066	0.3185	0.5176	0.2119	0.3493
KAN-GM-CPI + M2 + ER + EPU	0.1737	0.3777	0.0729	0.2081	0.2293	0.4719	0.1363	0.2792

Table 8. The performance of volatility forecasting models in the post-pandemic period.

	SP500				N225			
Model	MAE	RMSE	MedAE	Mean value	MAE	RMSE	MedAE	Mean value
GARCH	1.0385	1.5420	0.6610	1.0805	0.7481	0.8456	0.7290	0.7742
GM-CPI	1.0209	1.5053	0.6357	1.0539	0.8077	0.9119	0.7744	0.8313
GM-M2	1.2254	1.6636	0.9008	1.2633	0.8093	0.9092	0.7919	0.8368
GM-ER	1.2254	1.4707	0.6242	1.1068	0.7045	0.8109	0.6805	0.7320
GM-EPU	1.0814	1.5417	0.7025	1.1085	0.7431	0.8392	0.7275	0.7699
GM-CPI + M2	1.2389	1.6489	0.8786	1.2555	0.7431	0.8314	0.7121	0.7622
GM-CPI + ER	1.4580	2.1818	0.8545	1.4981	0.6961	0.8372	0.6318	0.7217
GM-CPI + EPU	1.0332	1.4519	0.7170	1.0674	0.8090	0.9230	0.8184	0.8501
GM-M2 + ER	2.4258	3.9385	1.1863	2.5169	0.8215	0.9200	0.8138	0.8518
GM-M2 + EPU	1.7183	2.0578	1.5450	1.7737	0.8045	0.9088	0.8085	0.8406
GM-ER + EPU	1.3181	1.8877	0.8215	1.3424	0.7185	0.8188	0.7022	0.7465
GM-CPI + M2 + ER	2.6903	4.2821	1.3868	2.7864	0.6668	0.8241	0.5707	0.6872
GM-CPI + M2 + EPU	1.1051	1.4975	0.7971	1.1333	0.7248	0.8298	0.7003	0.7516
GM-CPI + ER + EPU	1.2102	1.8595	0.7494	1.2730	0.9840	1.2035	0.8719	1.0198
GM-M2 + ER + EPU	1.9826	2.9932	1.2904	2.0888	0.8244	0.9439	0.8162	0.8615
GM-CPI + M2 + ER + EPU	1.3875	2.0710	0.8231	1.4272	0.8163	0.9826	0.7242	0.8410
KAN-GM-CPI	0.3904	0.6371	0.2994	0.4423	0.2090	0.4099	0.0746	0.2312
KAN-GM-M2	0.3513	0.6524	0.2064	0.4034	0.2383	0.3612	0.1824	0.2606
KAN-GM-ER	0.3674	0.6516	0.2572	0.4254	0.2492	0.3681	0.1921	0.2698
KAN-GM-EPU	0.3765	0.6471	0.2541	0.4259	0.2638	0.3715	0.2168	0.2841
KAN-GM-CPI + M2	0.3760	0.6343	0.2884	0.4329	0.2148	0.3674	0.1273	0.2365
KAN-GM-CPI + ER	0.4018	0.6486	0.3325	0.4610	0.2392	0.3695	0.1833	0.2640
KAN-GM-CPI + EPU	0.5052	0.7151	0.4531	0.5578	0.2501	0.3757	0.1987	0.2748
KAN-GM-M2 + ER	0.4634	0.7323	0.2980	0.4979	0.2327	0.3637	0.1839	0.2601
KAN-GM-M2 + EPU	0.3831	0.6571	0.2661	0.4355	0.2728	0.3708	0.2458	0.2964
KAN-GM-ER + EPU	4.7527	6.9157	4.1899	5.2861	0.2547	0.3675	0.2184	0.2802
KAN-GM-CPI + M2 + ER	0.4107	0.6649	0.3180	0.4645	0.2083	0.3759	0.1040	0.2294
KAN-GM-CPI + M2 + EPU	0.3911	0.6659	0.2584	0.4384	0.2547	0.3680	0.2009	0.2745
KAN-GM-CPI + ER + EPU	0.5972	0.8105	0.5005	0.6361	0.3386	0.4196	0.3207	0.3596
KAN-GM-M2 + ER + EPU	0.9493	1.3210	0.6398	0.9700	0.2938	0.3924	0.2524	0.3129
KAN-GM-CPI + M2 + ER + EPU	0.4445	0.6738	0.3602	0.4928	0.3012	0.3854	0.2856	0.3241

error indicators were significantly better than the traditional GARCH model and the basic GM model. Specifically, in the pre-epidemic sample (2009–2019), all KAN-GM variants achieved more accurate forecasting results; secondly, and more importantly, in the post-epidemic sample (2020–2023), the model also maintained stable forecasting performance, a finding that strongly verifies the model's ability to adapt to structural changes caused by the COVID-19 shock. Finally, the model's dual robust performance in normal economic environments and crisis periods not only confirms the reliability of its predictive effectiveness but also shows that it has unique advantages in capturing the nonlinear relationship between macroeconomic factors and market fluctuations.

5. Empirical performance of foreign exchange volatility forecasting models

This part aims to evaluate the applicability and predictive effectiveness of innovative forecasting models in the foreign exchange market. Based on two representative indicators, the US dollar index and the JPY/US exchange rate, this study systematically compares the forecasting performance of the traditional GARCH model, the GM model and the KAN-GM model.

In Table 9, the empirical analysis shows that the GM model optimized by the KAN algorithm shows significant advantages in forecasting accuracy: in terms of the three key evaluation indicators of MAE, RMSE and MedAE, the forecast error of the KAN-GM model is reduced by 60%–70% compared with the traditional model, among which the KAN-GM-EPU model integrating the economic policy uncertainty (EPU) factor performs best. Further research finds that: (1) the marginal contribution of the EPU factor to forecasting accuracy is significantly higher than that of the money supply (M2) factor; (2) the nonlinear modeling method can more effectively capture the complex characteristics of exchange rate fluctuations; (3) policy uncertainty has a greater explanatory power for short-term exchange rate fluctuations than traditional macroeconomic variables. These findings not only provide a better modeling framework for exchange rate forecasting, but also provide new empirical evidence for understanding the fluctuation mechanism of the foreign exchange market.

6. Comparison of volatility prediction between LSTM and GARCH type models

Since the input data sample size is large and the neural network model is highly random, to make the model better capture the data features and better compare the prediction results of different models, the data is divided into training set and test set in a ratio of 8:2. The hidden layer of the LSTM model is set to two layers, the number of memory units in the first layer is set to twice the number of input features, that is, 22, and relu is used as the activation function. The optimizer uses RMSprop, the learning rate is 0.01, the loss function is MAE, the batch size is set to 32, and the epoch is 30. In addition, a dropout layer is added to prevent overfitting, and its value is 0.1 (Song et al., 2023).

This section examines the performance differences of LSTM, GARCH and its improved models (including GM and KAN-GM) in the volatility forecasting of SP 500 and N225 through a systematic comparative analysis. To keep the research focus clear, we specifically selected two representative combinations with the largest average loss in the GM and KAN-GM models for key analysis.

In Table 10, the empirical results show that the prediction performance of the LSTM model is significantly weaker than all other benchmarks under the maximum average loss scenario. Specifically, in the forecast of the SP 500 index, the RMSE index of the LSTM model reached 0.5795, which is 19.8

Table 9. Comparison of error indicators of forex volatility forecasting models.

	US dollar index				JPY/USD			
Model	MAE	RMSE	MedAE	Mean value	MAE	RMSE	MedAE	Mean value
GARCH	0.0960	0.1683	0.0595	0.1079	0.2552	0.4841	0.1095	0.2829
GM-M2	0.0913	0.1650	0.0591	0.1052	0.2563	0.4862	0.1101	0.2842
GM-EPU	0.0928	0.1733	0.0612	0.1091	0.2574	0.4833	0.1141	0.2849
GM-M2 + EPU	0.0990	0.1765	0.0663	0.1140	0.2586	0.4855	0.1159	0.2867
KAN-GM-M2	0.0395	0.0733	0.0212	0.0447	0.1561	0.4947	0.0338	0.2282
KAN-GM-EPU	0.0378	0.0721	0.0209	0.0436	0.0791	0.2018	0.0317	0.1042
KAN-GM-M2 + EPU	0.0386	0.0718	0.0212	0.0439	0.0895	0.2033	0.0510	6.1146

Table 10. LSTM, GARCH, and GM/KAN-GM (worst performance) prediction error.

	SP500					N225			
Model	MAE	RMSE	MedAE	Mean value	Model	MAE	RMSE	MedAE	Mean value
LSTM	0.4178	0.5795	0.3217	0.4397	LSTM	0.376	0.5299	0.2698	0.3919
GARCH	0.2743	0.4835	0.1516	0.3031	GARCH	0.2784	0.3976	0.2159	0.2973
GM-EPU	0.2735	0.4837	0.1503	0.3025	GM-ER + EPU	0.2889	0.4025	0.2243	0.3052
KAN-GM-M2 + ER + EPU	0.2673	0.4826	0.1416	0.2972	KAN-GM-ER + EPU	0.2844	0.3973	0.2288	0.3035

percentage points higher than the worst-performing GM-EPU model; its MAE index is 52.3% higher than the benchmark GARCH model. Similarly, in the forecast of the Nikkei 225 index, the MedAE and average error of the LSTM model are 17.9% and 31.8% higher than the best benchmark model, respectively. These statistically significant differences fully demonstrate that in the absence of a specifically optimized design for low-frequency macro variables, the LSTM model is not only unable to surpass the time-tested traditional econometric models, but its forecasting accuracy is even difficult to reach the level of the most basic GARCH model.

7. Conclusion

This study addresses a research gap in the application of low-frequency macroeconomic variables in volatility forecasting using machine learning. Unlike existing literature that primarily employs traditional econometric models for feature extraction in machine learning or deep learning, this study takes a reverse approach. It combines the KAN with the GM model to enhance the forecasting performance of traditional econometric models through the nonlinear feature extraction capabilities of deep learning.

Through experiments, the effectiveness of this approach is verified: the KAN-GM model significantly outperforms traditional GARCH and GM models in out-of-sample forecasting for the SP500 and N225 indices, particularly in terms of MAE and MedAE indicators. The MCS test results further verified this finding. At a confidence level of 95%, the KAN-GM model was continuously retained in the optimal model set. This statistical inference result was highly consistent with the evaluation conclusion based on the loss function, jointly confirming the effectiveness of the model improvement from different dimensions. Additionally, integrating multiple low-frequency macroeconomic variables (e.g., CPI, M2, EPU, and exchange rate) further enhances forecasting accuracy and robustness. This finding not only highlights the power of deep learning techniques in capturing complex nonlinear features but also demonstrates that integrating these techniques with traditional econometric models can significantly improve the accuracy and stability of volatility forecasts.

In addition, this study confirmed that the KAN-GM model maintained stable forecasting performance under major external shocks through a comparative analysis of two subsamples before and after the COVID-19 epidemic. In the pre-epidemic samples, all KAN-GM variants showed more accurate forecasting effects; in the post-epidemic samples, the model also performed well, verifying its adaptability to structural changes. This dual robust performance in normal economic environments and crisis periods highlights the unique advantage of the model in capturing the nonlinear relationship between macroeconomic factors and market fluctuations.

In addition, in foreign exchange market applications, empirical results based on the US dollar index and JPY/US exchange rate show that the KAN-GM model has the lowest forecast error compared with traditional models, among which the KAN-GM-EPU model with EPU factor performs best. In addition, this study also systematically compares the forecasting performance of LSTM and GARCH models. The results show that the forecasting performance of the LSTM model is significantly weaker than that of other competing models.

This innovative approach offers a fresh perspective and theoretical foundation for volatility prediction research, paving the way for future studies in quantitative finance, particularly when addressing high-dimensional and complex economic variables. By leveraging the strengths of deep learning alongside traditional econometric models, this framework effectively captures long-term trends and nonlinear dynamics in financial markets. It equips market participants and policymakers with more accurate volatility forecasting tools, enabling them to better manage market risks and uncertainties.

Despite the significance of this study's findings, certain limitations remain. The analysis employs a fixed out-of-sample evaluation time window and does not test the model's adaptability under varying market conditions (e.g., economic crises or policy changes). Future research could explore the robustness of the model by implementing a rolling window approach or extending the analysis to other markets.

Disclosure statement

No potential conflict of interest was reported by the author(s).

Notes on contributors

Liu Ting: Conceptualization, Methodology, Formal analysis, Investigation, Writing - Original Draft, Visualization. **Weichong Choo:** Validation, Supervision, Resources. **Han Xinping:** Data Curation, Software. **Le Li:** Project administration, Writing - Reviewing and Editing.

References

Amendola, A., Candila, V., & Gallo, G. M. (2021). Choosing the frequency of volatility components within the Double Asymmetric GARCH–MIDAS–X model. *Econometrics and Statistics*, *20*, 12–28. https://doi.org/10.1016/j.ecosta.2020.11.001

Amirshahi, B., & Lahmiri, S. (2023). Hybrid deep learning and GARCH-family models for forecasting volatility of cryptocurrencies. *Machine Learning with Applications*, *12*, 100465. https://doi.org/10.1016/j.mlwa.2023.100465

Asgharian, H., Hou, A. J., & Javed, F. (2013). The importance of the macroeconomic variables in forecasting stock return variance: A GARCH-MIDAS approach. *Journal of Forecasting*, *32*(7), 600–612. https://doi.org/10.1002/for.2256

Asravor, R. K., & Fonu, P. D. D. (2021). Dynamic relation between macroeconomic variable, stock market returns and stock market development in Ghana. *International Journal of Finance Economics*, *26*(2), 2637–2646. https://doi.org/10.1002/ijfe.1925

Baker, S. R., Bloom, N., & Davis, S. J. (2016). Measuring economic policy uncertainty. *The Quarterly Journal of Economics*, *131*(4), 1593–1636. https://doi.org/10.1093/qje/qjw024

Bazrkar, M. J., & Hosseini, S. (2023). Predict stock prices using supervised learning algorithms and particle swarm optimization algorithm. *Computational Economics*, *62*(1), 165–186. https://doi.org/10.1007/s10614-022-10273-3

Bollerslev, T. (1986). Generalized autoregressive conditional heteroskedasticity. *Journal of Econometrics*, *31*(3), 307–327. https://doi.org/10.1016/0304-4076(86)90063-1

Brooks, S. (1998). Markov chain Monte Carlo method and its application. *Journal of the Royal Statistical Society: Series D (the Statistician)*, *47*(1), 69–100. https://doi.org/10.1111/1467-9884.00117

Camilleri, S. J., Scicluna, N., & Bai, Y. (2019). Do stock markets lead or lag macroeconomic variables? Evidence from select European countries. *The North American Journal of Economics and Finance*, *48*, 170–186. https://doi.org/10.1016/j.najef.2019.01.019

Cheng, H., & Shi, Y. (2020). Forecasting China's stock market variance. *Pacific-Basin Finance Journal*, *64*, 101421. https://doi.org/10.1016/j.pacfin.2020.101421

Chinzara, Z. (2011). Macroeconomic uncertainty and conditional stock market volatility in South Africa. *South African Journal of Economics*, *79*(1), 27–49. https://doi.org/10.1111/j.1813-6982.2011.01262.x

Cizeau, P., Liu, Y., Meyer, M., Peng, C.-K., & Stanley, H. E. (1997). Volatility distribution in the S&P500 stock index. *Physica A: Statistical Mechanics and Its Applications*, *245*(3-4), 441–445. https://doi.org/10.1016/S0378-4371(97)00417-2

Engle, R. F., Ghysels, E., & Sohn, B. (2013). Stock market volatility and macroeconomic fundamentals. *Review of Economics and Statistics*, *95*(3), 776–797. https://doi.org/10.1162/REST_a_00300

Engle, R. F., & Patton, A. J. (2007). *What good is a volatility model? Forecasting volatility in the financial markets* (pp. 47–63). Elsevier.

Engle, R. F., & Rangel, J. G. (2008). The spline-GARCH model for low-frequency volatility and its global macroeconomic causes. *The Review of Financial Studies*, *21*(3), 1187–1222. https://doi.org/10.1093/rfs/hhn004

Ersin, Ö. Ö., Gül, M., & Aşik, B. (2022). Are the policy uncertainty and cli'effective' indicators of volatility? GARCH-MIDAS analysis of the g7 stock markets. *Economic Computation Economic Cybernetics Studies Research*, *56*(1), 141–158. https://doi.org/10.24818/18423264/56.1.22.09

Ghani, M., Guo, Q., Ma, F., & Li, T. (2022). Forecasting Pakistan stock market volatility: Evidence from economic variables and the uncertainty index. *International Review of Economics Finance*, *80*, 1180–1189. https://doi.org/10.1016/j.iref.2022.04.003

Ghysels, E., Sinko, A., & Valkanov, R. (2007). MIDAS regressions: Further results and new directions. *Econometric Reviews*, *26*(1), 53–90. https://doi.org/10.1080/07474930600972467

Gong, X., Zhang, W., Wang, J., & Wang, C. (2022). Investor sentiment and stock volatility: New evidence. *International Review of Financial Analysis*, *80*, 102028. https://doi.org/10.1016/j.irfa.2022.102028
Guidolin, M., Hyde, S., McMillan, D., & Ono, S. (2009). Non-linear predictability in stock and bond returns: When and where is it exploitable? *International Journal of forecasting*, *25*(2), 373–399. https://doi.org/10.1016/j.ijforecast.2009.01.002
Hajilee, M., & Nasser, O. M. (2014). Exchange rate volatility and stock market development in emerging economies. *Journal of Post Keynesian Economics*, *37*(1), 163–180. https://doi.org/10.2753/PKE0160-3477370110
Han, H., Liu, Z., Barrios Barrios, M., Li, J., Zeng, Z., Sarhan, N., & Awwad, E. M. (2024). Time series forecasting model for non-stationary series pattern extraction using deep learning and GARCH modeling. *Journal of Cloud Computing*, *13*(1), 2. https://doi.org/10.1186/s13677-023-00576-7
Hansen, P. R., Lunde, A., & Nason, J. M. (2011). The model confidence set. *Econometrica*, *79*(2), 453–497. https://doi.org/10.3982/ECTA5771
Khan, W. A., Javed, M. A., Shahzad, N., Sheikh, Q., Saddique, S., Riaz, M., & Batool, S. (2014). Impact of macroeconomics variable on the stock market index: A study from Pakistan. *International Journal of Accounting and Financial Reporting*, *4*(2), 258. http://dx.doi.org/10.5296/ijafr.v4i2.6483
Kou, G., Olgu Akdeniz, Ö., Dinçer, H., & Yüksel, S. (2021). Fintech investments in European banks: A hybrid IT2 fuzzy multidimensional decision-making approach. *Financial Innovation*, *7*(1), 39. https://doi.org/10.1186/s40854-021-00256-y
Lahmiri, S. (2020). A predictive system integrating intrinsic mode functions, artificial neural networks, and genetic algorithms for forecasting S&P500 intra-day data. *Intelligent Systems in Accounting, Finance and Management*, *27*(2), 55–65. https://doi.org/10.1002/isaf.1470
Li, T., Ma, F., Zhang, X., & Zhang, Y. (2020). Economic policy uncertainty and the Chinese stock market volatility: Novel evidence. *Economic Modelling*, *87*, 24–33. https://doi.org/10.1016/j.econmod.2019.07.002
Li, Y., Ma, F., Zhang, Y., & Xiao, Z. (2019). Economic policy uncertainty and the Chinese stock market volatility: New evidence. *Applied Economics*, *51*(49), 5398–5410. https://doi.org/10.1080/00036846.2019.1613507
Liu, M., Lee, C.-C., & Choo, W.-C. (2021). The role of high-frequency data in volatility forecasting: Evidence from the China stock market. *Applied Economics*, *53*(22), 2500–2526. https://doi.org/10.1080/00036846.2020.1862747
Liu, M., Taylor, J. W., & Choo, W.-C. (2020). Further empirical evidence on the forecasting of volatility with smooth transition exponential smoothing. *Economic Modelling*, *93*, 651–659. https://doi.org/10.1016/j.econmod.2020.02.021
Liu, Z., Wang, Y., Vaidya, S., Ruehle, F., Halverson, J., Soljačić, M., Hou, T. Y., & Tegmark, M. (2024). Kan: Kolmogorov–Arnold networks, arXiv preprint, arXiv:2404.19756. https://doi.org/10.48550/arXiv.2404.19756
Ljung, G. M., & Box, G. E. (1979). The likelihood function of stationary autoregressive-moving average models. *Biometrika*, 66(2), 265–270. https://doi.org/10.1093/biomet/66.2.265
Ma, F., Lu, X., Yang, K., & Zhang, Y. (2019a). Volatility forecasting: Long memory, regime switching and heteroscedasticity. *Applied Economics*, *51*(38), 4151–4163. https://doi.org/10.1080/00036846.2019.1589645
Ma, Y., Ji, Q., & Pan, J. (2019b). Oil financialization and volatility forecast: Evidence from multidimensional predictors. *Journal of Forecasting*, *38*(6), 564–581. https://doi.org/10.1002/for.2577
Manera, M., & Forte, G. (2002). Forecasting volatility in European stock markets with non-linear GARCH models.
McLeod, A. I., & Li, W. K. (1983). Diagnostic checking ARMA time series models using squared-residual autocorrelations. *Journal of Time Series Analysis*, 4(4), 269–273. https://doi.org/10.1111/j.1467-9892.1983.tb00373.x
Mishra, A., & Debata, B. (2020). Does economic policy uncertainty matter for stock market volatility? In A. K. Mishra, V. Arunachalam, S. Mohapatra, & D. Olson (Eds.), *The Financial Landscape of Emerging Economies: Current State, Challenges and Solutions* (pp. 45–53). Gewerbestrasse 11, 6330 Cham, Switzerland: Springer.
Mroua, M., & Trabelsi, L. (2020). Causality and dynamic relationships between exchange rate and stock market indices in BRICS countries: Panel/GMM and ARDL analyses. *Journal of Economics, Finance and Administrative Science*, *25*(50), 395–412. https://doi.org/10.1108/JEFAS-04-2019-0054
Okechukwu, I. A., Mbadike, N. S., Geoffrey, U., & Ozurumba, B. A. (2019). Effects of exchange rate, interest rate, and inflation on stock market returns volatility in Nigeria. *International Journal of Management Science and Business Administration*, *5*(6), 38–47. https://doi.org/10.18775/ijmsba.1849-5664-5419.2014.56.1005
Park, B. J. (2002). An outlier robust GARCH model and forecasting volatility of exchange rate returns. *Journal of Forecasting*, *21*(5), 381–393. https://doi.org/10.1002/for.827
Poon, S.-H., & Granger, C. W. J. (2003). Forecasting volatility in financial markets: A review. *Journal of Economic Literature*, *41*(2), 478–539. https://doi.org/10.1257/002205103765762743
Rayadurgam, V. C., & Mangalagiri, J. (2023). Does inclusion of GARCH variance in deep learning models improve financial contagion prediction? *Finance Research Letters*, *54*, 103707. https://doi.org/10.1016/j.frl.2023.103707
Sadorsky, P. (2005). Stochastic volatility forecasting and risk management. *Applied Financial Economics*, *15*(2), 121–135. https://doi.org/10.1080/0960310042000299926
Schwert, G. W. (1989). Why does stock market volatility change over time?*The Journal of Finance*, *44*(5), 1115–1153. https://doi.org/10.1111/j.1540-6261.1989.tb02647.x
Song, Y., Tang, X., Wang, H., & Ma, Z. (2023). Volatility forecasting for stock market incorporating macroeconomic variables based on GARCH-MIDAS and deep learning models. *Journal of Forecasting*, *42*(1), 51–59. https://doi.org/10.1002/for.2899

Su, Z., Fang, T., & Yin, L. (2019). Understanding stock market volatility: What is the role of US uncertainty? *The North American Journal of Economics and Finance*, *48*, 582–590. https://doi.org/10.1016/j.najef.2018.07.014

Tsay, R. S. (2005). In D. J. Balding, N. A. C. Cressie, & N. I. Fisher (Eds.), *Analysis of financial time series* (Vol. 638 USA: John Wiley and Sons.

Wang, L., Ma, F., Liu, J., & Yang, L. (2020). Forecasting stock price volatility: New evidence from the GARCH-MIDAS model. *International Journal of Forecasting*, *36*(2), 684–694. https://doi.org/10.1016/j.ijforecast.2019.08.005

Wei, Y., Bai, L., Yang, K., & Wei, G. (2021). Are industry-level indicators more helpful to forecast industrial stock volatility? Evidence from Chinese manufacturing purchasing managers index. *Journal of Forecasting*, *40*(1), 17–39. https://doi.org/10.1002/for.2696

Wu, C., Wang, X., Luo, S., Shan, J., & Wang, F. (2020). Influencing factors analysis of crude oil futures price volatility based on mixed-frequency data. *Applied Sciences*, *10*(23), 8393.

Wu, X., Liu, T., & Xie, H. (2021). Economic policy uncertainty and Chinese stock market volatility: A CARR-MIDAS approach. *Complexity*, *2021*, 1–10. https://doi.org/10.1155/2021/4527314

Wu, X., Yin, X., & Mei, X. (2022). Forecasting the volatility of European union allowance futures with climate policy uncertainty using the EGARCH-MIDAS model. *Sustainability*, *14*(7), 4306. https://doi.org/10.3390/su14074306

Wu, X., Zhao, A., & Cheng, T. (2023). A real-time GARCH-MIDAS model. *Finance Research Letters*, *56*, 104103. https://doi.org/10.1016/j.frl.2023.104103

Xu, Y., Wang, J., Chen, Z., & Liang, C. (2021). Economic policy uncertainty and stock market returns: New evidence. *The North American Journal of Economics and Finance*, *58*, 101525. https://doi.org/10.1016/j.najef.2021.101525

Yaya, O. S., Ogbonna, A. E., & Vo, X. V. (2022). Oil shocks and volatility of green investments: GARCH-MIDAS analyses. *Resources Policy*, 78, 102789. https://doi.org/10.1016/j.resourpol.2022.102789

Yu, H., Fang, L., & Sun, W. (2018). Forecasting performance of global economic policy uncertainty for volatility of Chinese stock market. *Physica A: Statistical Mechanics and its Applications*, *505*, 931–940. https://doi.org/10.1016/j.physa.2018.03.083

Yu, X., & Huang, Y. (2021). The impact of economic policy uncertainty on stock volatility: Evidence from GARCH–MIDAS approach. *Physica A: Statistical Mechanics and Its Applications*, *570*, 125794. https://doi.org/10.1016/j.physa.2021.125794

Yu, Y., Lin, Y., Hou, X., & Zhang, X. (2023). Novel optimization approach for realized volatility forecast of stock price index based on deep reinforcement learning model. *Expert Systems with Applications*, *233*, 120880. https://doi.org/10.1016/j.eswa.2023.120880